

Into the dust: Radio luminosity Calibrations of SFR in Distant Galaxies

Thando Mothogoane - Ph.D student at the University of Johannesburg (UJ)

Email: gmothogoane@uj.ac.za

Dr. S Kolwa (UJ), Dr. K Thorat (University of Pretoria), Prof. S Razzaque (UJ)



X : @Thando_Mo29

Star formation within Deep Radio Surveys

We investigate the **1.4 GHz luminosity ($L_{1.4 \text{ GHz}}$) vs. far-infrared (FIR) luminosity (L_{FIR}) and $L_{1.4 \text{ GHz}}$ vs. star formation rate (SFR) correlations** for radio selected sources that have optical and near-infrared (NIR) detections and are traced up to $z \sim 6$. Using deep radio continuum images from the MeerKAT International GHz Tiered Extragalactic Exploration (MIGHTEE) survey, we study the above correlations in 5223 galaxies in the Early Science COSMOS field (Jarvis et al. 2016). The goal of this work is to:

- Determine whether the non-jetted and radio-quiet active galactic nuclei (RQ AGN) follow the radio-FIR correlation
- Calibrate the SFR- $L_{1.4 \text{ GHz}}$ relation for radio emitting galaxies at high redshifts

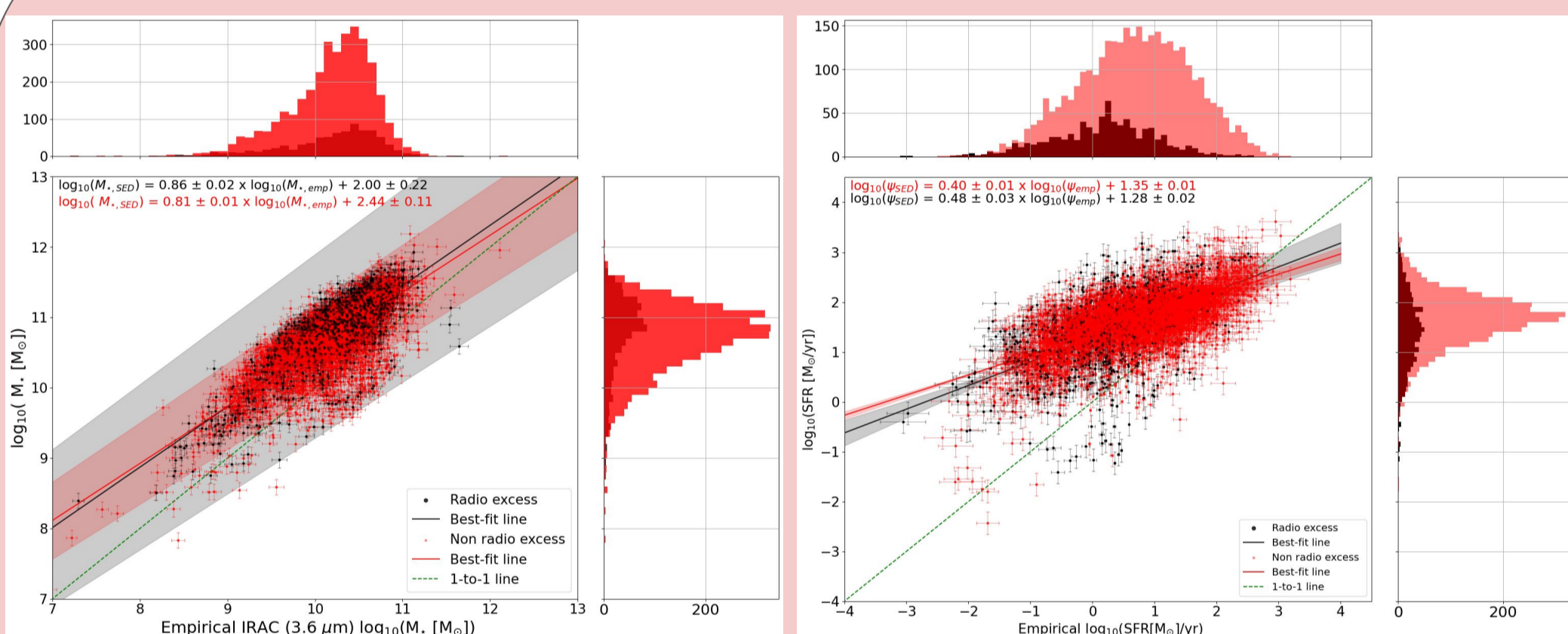
Constraining galaxy properties

In this study, we constrain the **stellar masses (M_*) and SFRs** of the radio selected galaxies using spectral energy distribution (SED) analysis. We employ the SED fitting code **MAGPHYS** (da Cunha et al. 2008) for this purpose.

To ensure the accuracy of our results, we compare the SED-derived M_* and SFRs with those obtained from empirical measurements. The empirical M_* were derived using a constant mass-to-light ratio of 0.47 (McGaugh & Schombert 2014). The empirical SFRs were obtained using the following equation from Kennicutt (1998),

$$\text{SFR} = \frac{L_{\text{FIR}}}{5.8 \times 10^9 L_{\odot}} \quad \text{where } L_{\text{FIR}} \text{ is the FIR luminosity.}$$

Feasibility check for M_* and SFR



We obtain a **positive correlation between the SED-derived and empirical** for both the M_* and SFRs. The slopes for the M_* (RE ~ 0.81 , unclassified ~ 0.79) and SFR (RE ~ 0.46 , unclassified ~ 0.44) are shallower than expected, but most SFRs fall within the 3σ region of error.

These MAGPHYS derived M_* and SFRs are consistent with the empirical measures, therefore they can be reliably used in the rest of the analysis.

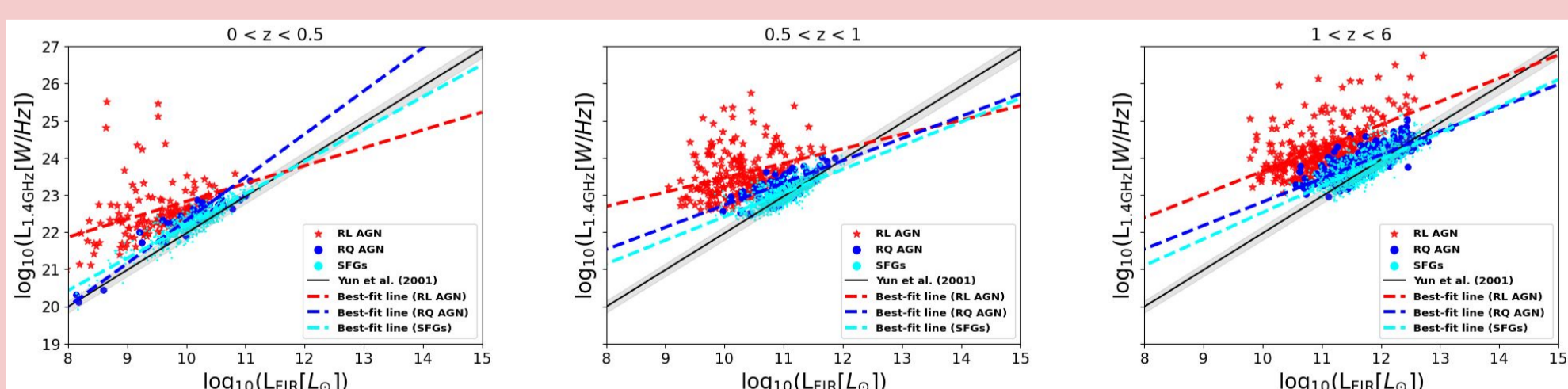
Mothogoane et al. (in prep)

$L_{\text{FIR}} - L_{1.4 \text{ GHz}}$ correlation

$$L_{\text{FIR}} = 4\pi d_L^2 S_{\text{FIR}} \quad \text{Where } d_L \text{ is the luminosity distance and } S_{\text{FIR}} \text{ is the FIR flux density}$$

$$L_{1.4 \text{ GHz}} = 4\pi d_L^2 \frac{S_{1.4 \text{ GHz}}}{(1+z)^{1+\alpha}}$$

Where $S_{1.4 \text{ GHz}}$ is the radio flux density at rest-frame frequency and α is the radio spectral index of -0.7 (Ibar et al. 2010)



SFGs and RQ AGN follow the correlation at $z < 0.5$. At higher redshifts ($z > 0.5$), radio luminosities increase slowly for SFGs and RQ AGN, while FIR luminosities increase significantly. RL AGN shows a significant deviation from the correlation across all the redshift ranges.

Radio observations

We use the MIGHTEE Early Science radio continuum data observed from a single pointing in the COSMOS field covering $\sim 1.6 \text{ deg}^2$ at 1.28 GHz. This data was optimised for higher sensitivity using the Briggs (1995) robustness parameter of 0.0 and the image have a thermal noise of $1.7 \mu\text{Jy/beam}$ (Heywood et al. 2022). Source finding was done using the PYTHON Blob Detector and Source Finder (Mohan & Rafferty 2015), which was configured with a peak brightness threshold of $5\sigma_{\text{local}}$ (where σ_{local} is the local background noise).

Multiwavelength data

- Optical data - HSC and CFHT surveys (Tanaka et al. 2017, Furusawa et al. 2016)
- NIR data - UltraVISTA (McCracken et al. 2012) and SPLASH (Steinhardt et al. 2014)
- The mid-infrared (MIR) - *Spitzer*/MIPS (Rieke et al. 2004)
- FIR data - *Herschel*/PACS (Poglitsch et al. 2010) and *Herschel*/SPIRE (Griffin et al. 2010)
- X-ray data - *Chandra* COSMOS-Legacy (Marchesi et al. 2016)

Radio source classifications

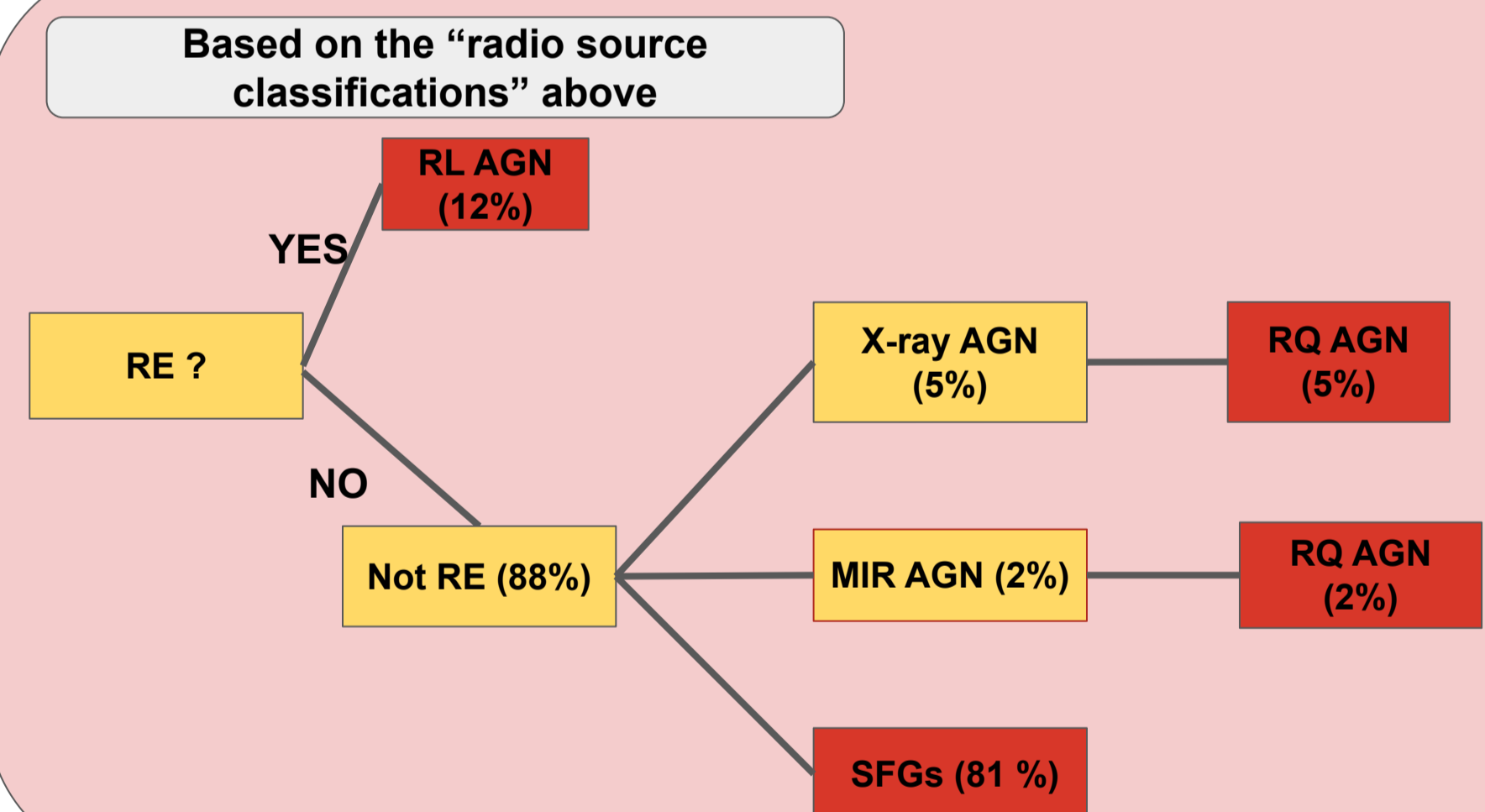
We use the following four diagnostics for our classifications:

- Radio excess (RE, infrared-radio ratio below 0.43 dex from Delvecchio et al. (2021))
- X-ray luminosity cut (X-ray AGN if $L_{\text{X-ray}} > 10^{42} \text{ erg s}^{-1}$, Szokoly et al. 2004)
- Mid-infrared color cut (MIR, Donley et al. 2012).

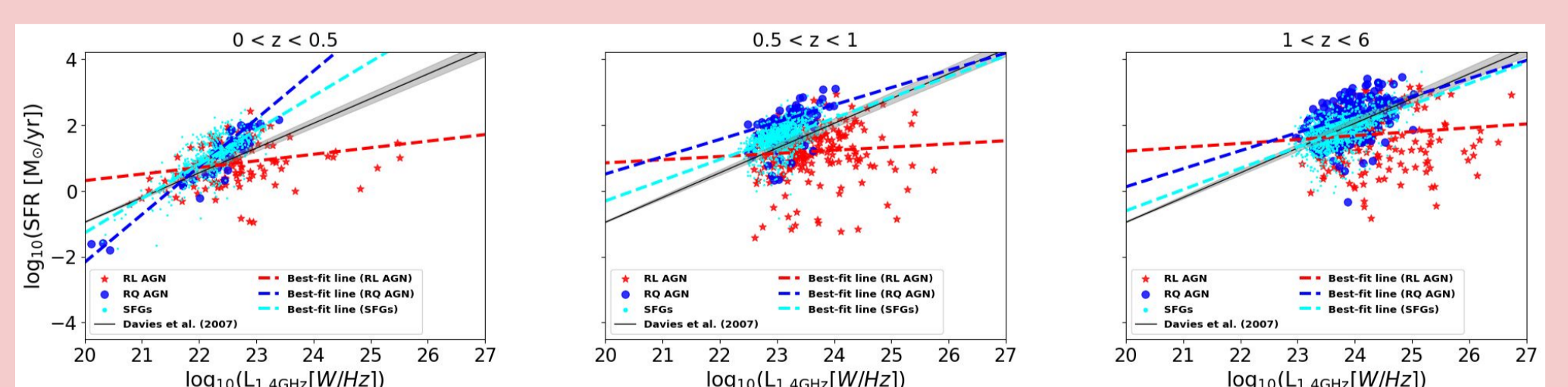
We then classify the MIGHTEE radio sources into the following seven classes:

- RL AGN (radio-loud AGN): RE
- RQ AGN: X-ray AGN, MIR AGN
- Star forming galaxy (SFGs) - if not RE, X-ray AGN, and MIR AGN

Classification scheme



Calibration of the SFR- $L_{1.4 \text{ GHz}}$ correlation



SFGs and RQ AGN show a positive correlation consistently up to $z < 6$, while RL AGN exhibits little to no correlation. At higher redshifts ($z > 0.5$), SFGs and RQ AGN experience an increase in SFR with a slow increase in radio luminosities. RL AGN show a high increase in radio luminosities with increasing redshift, while SFR increases slowly. The flat best-fit line for RL AGN indicates a decoupling for SFR and radio luminosities.

Preliminary Conclusions

We find that the **RQ AGN follow the FIR-radio relation up to $z < 6$** similar to SFGs as studied by Yun et al. (2001). This preliminary result implies that **radio emission in the majority of RQ AGN from our sample may be tracing star-formation**. The correlation between SFR and $L_{1.4 \text{ GHz}}$ for RQ AGN is positive across all the redshift ranges and the calibration is similar to that of SFGs. At $z > 0.5$ in both the correlations, L_{FIR} and SFRs increase significantly for RQ AGN. **This implies that radio luminosities can be reliably used as dust-free measures of star-formation in galaxies up to $z \sim 6$** . RL AGN deviates from the $L_{\text{FIR}} - L_{1.4 \text{ GHz}}$ and SFR - $L_{1.4 \text{ GHz}}$ relations, **this suggests that the radio luminosity in RL AGN is dominated by AGN activity rather than star-formation.**